A comparative molecular field analysis of cytotoxic beta-carboline analogs

Xue-rui HOU, Qi CHEN, Ri-hui CAO, Wen-lie PENG, An-long XU[1]

Department of Biochemistry and Center for Biopharmaceutical Research, College of Life Sciences, Sun Yat-sen University, Guangzhou 510275, China

KEY WORDS beta-carbolines; quantitative structure-activity relationship; alkaloids

ABSTRACT

AIM: To derive a model that could be used in drug design. **METHODS:** Beta-carbolines are reported to have antitumor activities on cultured cancer cell lines. A comparative molecular field analysis (CoMFA) was undertaken to elucidate the correlation of cytotoxities and structural parameters of 16 beta-carboline analogs (**1**-**16**). The compound **12** was finally used as a template for the other compounds in the dataset because of its highest biological activity. **RESULTS:** The CoMFA applied to the final alignment resulted in a q^2_{cv} of 0.656 and it showed that the steric fields contributed 43.3 % of the model information while the electrostatic fields represented the other 56.7 %. **CONCLUSION:** Three designed compounds, which were predicted to have high, moderate and low activities respectively, were synthesized. The IC_{50} values of these compounds indicated the significance of the analysis in this study. The model derived from the current study could be further used in design for more active compounds.

INTRODUCTION

Beta-carbolines have been reported to possess significant antitumor activities[1,4,6,9,17], in addition these compounds are widely studied for their bioactivity in antibacterial, anti-radialization, anti-trypanosome, and neural activities as well as mutagenic and co-mutagenic properties. Also they are potent and specific inhibitors of cyclin-dependent kinases[2,3,5,8-10,12-17]. The extracts containing beta-carbolines from the plant *Peganum harmala* have been widely used in Northwest China as a very potent antitumor folk medicine, in which the main effective contents are beta-carboline alkaloids such as harmaline, harmine, harmalol, and harman[1-5]. Aboriginal in South Africa use it to ease pain and hyperkinesias[7]. Also the plant *Peganum harmala* is used as medicine for cancers of digestive system[7]. Evidence shows that beta-carbolines interact with DNA but it remains unclear about the way these compounds bind to the receptor and how they operate[8].

As no clear receptor-ligand interaction is available, in this study the comparative molecular field analysis (CoMFA) is chosen as a valuable tool to study the 3D-QSAR[18] within a set of aligned ligands. This tridimensional grid-based QSAR technique correlates variations of biological activities with variation of electrostatic or steric fields. If a validated QSAR is obtained, it is first possible to visualize the results graphically, ie, the regions where a variation of the electrostatic or steric potentials has been correlated with a variation of the biological activities. The key of such a validated CoMFA model is the ability to predict the activity of new chemi-

[1] Correspondence to Prof An-long XU. Phn 86-20-8411-3655. Fax 86-20-8403-8377. E-mail ls36@zsu.edu.cn
Received 2003-07-21 Accepted 2004-02-06

cal structures in an effort to guide the synthesis of new bioactive compounds. Many reports have shown the value of 3D-QSAR techniques such as CoMFA in the design of drug molecules with unclear receptor.

The study on the structure-antitumor activity relationship of beta-carbolines was initiated in the report. Both CoMFA and QSAR programs we used were provided in the SYBYL software package version 6.5 (Tripos Co Ltd, USA). Three designed compounds were synthesized and tested to verify the validity of the gained model.

MATERIALS AND METHODS

Chemical The compounds of the test set were prepared from the initial structure of harmine (scheme 1).

Synthesis of compound 17: 7-methoxy-1-methyl-9-ethyl-pyrido [3, 4-b] indole hydrogen chloride A mixture of harmine (2.12 g, 10 mmol), DMF (50 mL), and THF (50 mL) were stirred at room temperature until clear, NaH (0.72 g, 30 mol) and CH_3I (4.5 mL, 60 mmol) were added. The mixture was refluxed for 2 h, then evaporated under reduced pressure. The resulting mixture was poured into H_2O (100 mL), and extracted with ethyl acetate (3×150 mL). The combined ethyl acetate extracts were washed with water and brine, then dried (Na_2SO_4), filtered and evaporated. After collection, the solid was dissolved in ethanol (30 mL) and added with concentrated HCl (5 mL). Then the mixture was evaporated and recrystallized from acetone to give a white solid in 92 % yield.

Synthesis of compound **18**: 7-methoxy-1-methyl-9-benzyl-pyrido [3, 4-b] indole hydrogen chloride A mixture of harmine (2.12 g, 10 mmol), DMF (50 mL), and THF (50 mL) were stirred at room temperature until clear, then NaH (0.72 g, 30 mol) and $C_6H_5CH_2I$ (8 mL) were added. The mixture was refluxed for 18 h, and then evaporated under reduced pressure. The resulting mixture was poured into ice-water (100 mL), and adjusted to pH 3 with HCl, then extracted with ethyl ether (2×100 mL). The aqueous phase was neutralized to pH 8 with saturated $NaHCO_3$ solution, and then was extracted with ethyl acetate. The combined ethyl acetate extracts were washed with water and brine, then dried (Na_2SO_4), filtered and evaporated. After collection, the solid was dissolved in ethanol (30 mL) and 5 mL concentrated HCl. The mixture was evaporated and recrystallized from acetone to give a white solid in 93 % yield.

Synthesis of compound **19**: 7-methoxy-1-methyl-9-hydroxyethyl-pyrido [3, 4-b] indole hydrogen chloride A mixture of harmine (2.12 g, 10 mmol), DMF (50 mL), and THF (50 mL) were stirred at room temperature until clear, and then NaH (0.72 g, 30 mol) and $HOCH_2CH_2I$ (5 mL) were added. The mixture was refluxed for 6 h, then evaporated under reduced pressure. The resulting mixture was poured into H_2O (100 mL), and extracted with ethyl acetate (3×150 mL). The combined ethyl acetate extracts were washed with water and brine, then dried (Na_2SO_4), filtered and evaporated. After collection, the solid was dissolved with ethanol (30 mL) and 5 mL concentrated HCl. The mixture was evaporated and recrystallized from ethanol resulting in a white solid in 60 % yield.

3D-QSAR

Compounds and measurement of cytotoxic activities Compounds in test set have been synthesized in our laboratory and their cytotoxic activities shown as IC_{50} values were tested through MTT method[27]. The pIC_{50} values used in CoMFA were described by Ishidda *et al*. All compounds used in this study were listed in Tab 1, and their structures were all energy-minimized and superim-posted based on the non-hydrogen atoms. Compound **17**, **18,** and **19** were served as a test set for the validation of our model and therefore were not included in the CoMFA analysis.

Scheme 1. Synthesis of compound 17, compound 18, and compound 19.

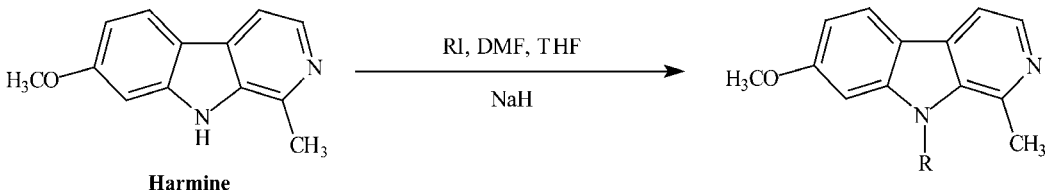

Harmine

1) RI=CH_3I compound **17** R=CH_3
2) RI=$C_6H_5CH_2I$ compound **18** R=$C_6H_5CH_2$
3) RI=$HOCH_2CH_2I$ compound **19** R=$HOCH_2CH_2$

Tab 1. Compounds and data used in the investigation.

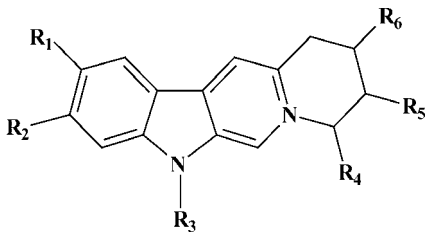

Compound	R_1	R_2	R_3	R_4	R_5	R_6	pIC_{50}
1	H	OCH_3	H	CH_3	---	H	1.756
2	H	OH	H	CH_3	---	H	1.476
3	H	OC_2H_5	H	CH_3	---	H	1.483
4	H	$OCH(CH_3)_2$	H	CH_3	---	H	1.287
5	H	$O(CH_2)_5\ CH_3$	H	CH_3	---	H	2.000
6	H	OAc	H	CH_3	---	H	1.444
7	H	OCH_3	CH_3	CH_3	---	H	1.81
8	H	OCH_3	C_2H_5	CH_3	---	H	1.767
9	H	OCH_3	C_4H_9	CH_3	---	H	1.565
10	H	H	H	CH_3	---	H	1.249
11	Br	OCH_3	H	CH_3	---	H	1.180
12	H	OCH_3	H	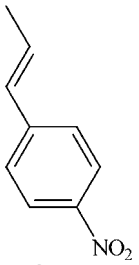	---	H	2.326
13	H	OCH_3	H	CH_3	NO	H_2	1.085
14	H	OCH_3	H	$(CH_2)_7\ CH_3$	H	COOH	0.889
15	H	OCH_3	H	$CH(C_2H_5)\ C_2H_5$	H	COOH	0.939
16				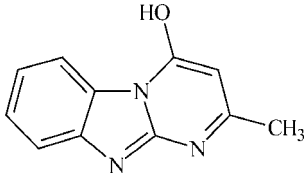			0.998
17	H	OCH_3	CH_3	CH_3	---	H	1.74
18	H	OCH_3	$C_6H_5CH_2$	CH_3	---	H	1.45
19	H	H	$C_6H_5CH_2$	H	---	COOH	1.08

Construction and optimization of the structures All the molecules were sketched on a Silicon Graphics IRIS workstation and optimized by methods of molecular dynamics. Simplex method and Powell method were used to optimize their structures in Tripos force field. Gasterger-Hückle charges and distance-based permittivity were selected and the gradient termination was 0.01 kcal/mol. Random search was used to get the low energy conformations of the molecules. Then the molecules were computed by methods of systemic search and simulate anneal which included 10 circles and the temperature ranged from 250 K to 1000 K to get the lowest and second lowest energy conformation. The descriptive electrostatic and steric components of the intermolecular interaction field were calculated as implemented in SYBYL using Coulomb and Lennard-Jones potentials, respectively.

Template selection Compound **10** was used as

a template first because of its simplest configuration. To use it as a template, it is important that the correct conformation state is used for the alignments. It was chosen by clustering and rigid body alignment of all conformations to the studied compounds. When CoMFA was finished, the q^2_{cv} was a negative one. Based on the CoMFA theory, it meant that the relativity was unreliable and the result was unreasonable. Alternatively, the most active compound **12** was used as a template for all the other compounds in the dataset.

Fit of the compounds Rms (root meat square) Fit and Field Fit were both used to fit the other compounds to the template-compound **12**. When rms Fit was used, all the atoms of the core frame were selected as fit sites. Based on the theory of field Fit[3], the steric and electrostatic force fields of all the molecules were fitted to that of the template. The final models grained by these two methods showed no obvious difference from each other, perhaps because of the rigidity of each compound structure. When the lowest energy conformation of compound **12** was used as the template, the rms fit was applied and the best result was obtained.

CoMFA The analysis was performed using an sp^3 carbon probe (C.3, charge +1.0) positioned at the lattice points (1 Å Increment) of a regular grid. Column filtering was set to 2.0 kal/mol, steric and electrostatic cutoffs to 30.0 kal/mol with smooth transition. The obtained data were regressed by a partial-least-squares (PLS) analysis to the target property pIC_{50} (-log IC_{50}). To check the statistical significance of the models, cross-validations by the "leave-one-out" method were performed. The optimal number of components was determined by the smallest standard error of prediction $s_{c/v}$. This value, which did not necessarily correspond to the highest q^2_{cv}, was used to derive the final QSAR model. The statistical data were summarized in Tab 2, and the plots of the predicted versus the experimental cytotoxic activities were shown in Fig 1.

RESULTS

CoMFA The steric and electronic force fields were checked. The PLS analysis of our aligned dataset yielded a non-cross validated r^2 of 0.984 and a cross-validated q^2 of 0.656 with $s_{c/v}$=0.058 using 16 compounds (Tab 2). The obtained experimental activities of the beta-carbolines correlated well with the results of our theoretical CoMFA model, with residuals near zero (Fig 1). To solve possible problems of the analysis arising from the absolute orientation of the molecules within the grid space, it is useful to translate and/or rotate the entire dataset within the lattice. This can be done manually by using the STATIC TRANSLATE or STATIC ROTATE commands in SYBYL. It was automated by providing a SPL script that systematically changed the position of all molecules in the dataset without changing their relative orientation. After each of 1296 reorientation steps, the PLS analysis was repeated. For our dataset and alignment, the translation and/or rotational variance of the CoMFA did not improve the model when applying a grid spacing of 1 Å. Neither modification of the CoMFA parameters, such as changing cutoff values for steric/electrostatic energies, nor changes of the field types, such as H-bond field, dipole moments, molecular weight and refractivity, neither resulted in im-

Tab 2. Summary of the CoMFA results.

Orientation validation	PLS (Leave-one-out)
Compounds	16
q^2 (cross validation)	0.656
r^2 (non-cross validation)	0.984
$s_{c/v}$	0.058
F	122.747
Fraction (steric/electro)	0.433/0.567
Grid increment	1 Å

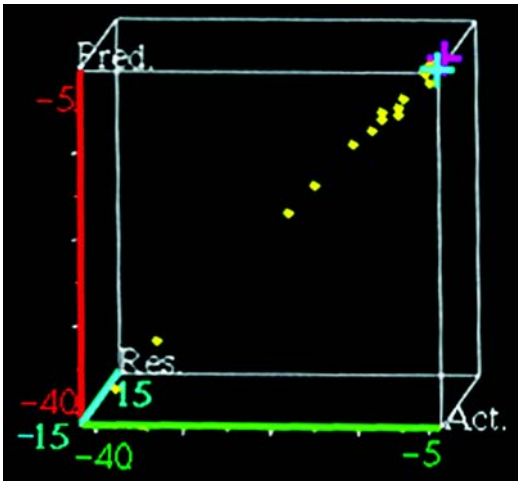

Fig 1. Predicted versus experimental cytotoxity for the beta-carbolines included in the dataset. The data for the best model after systematic orientation of the aligned molecules within the lattice is shown. The q^2_{cv} value is 0.656, in the case of the nonvalidated prediction r^2=0.984, standard error of estimate s=0.058.

provement of the model.

Graphical interpretation of the results The tridimensional representation of the CoMFA data as contour plots allows the correlation of experimentally determined cytotoxicity data with changes in steric (green/yellow) or electrostatic (blue/red) properties (Fig 2). As a guide, the template compound **12** is shown embedded into the final field as a representative example.

Steric contributions The steric contribution to the overall molecular field is only 43.3 % and therefore is difficult to interpret. The yellow surface located in R_5 and R_2 parts indicates a region where steric contributions are unfavored. This can be observed in compound **2** and **6**. The R_2 area of compound **2** is smaller than that of compound **6**, so the pIC_{50} of compound **2** is higher than that of compound **6**. However, it should be noticed that not all bulky substitutions decrease the cytotoxic activities in case of compound **13**, **14**, and **15**.

Electrostatic contributions The electrostatic contribution to the overall molecular field is 56.7 %. In R_2 area of the molecules, three red regions dominate the electrostatic field. It means that there are regions where a negative potential is favorable for pIC_{50}. This principal behavior can be observed in compound **4**, **5** and **10** whose R_2 areas all are positive in potential. In R_6 area, there are two blue regions whose mean negative potential is unfavorable for pIC_{50}. The principle behavior can be seen in the R_6 areas of compound **14** and **15**.

Application on test compounds Compound **17**, **18**, and **19** are synthesized and the CoMFA model was used to predict their cytotoxic activities. The experimental versus the calculated pIC_{50} values were shown in Tab 3. The experimental values of compound **17** and **18** fitted the calculated pIC_{50} values well though the residual of compound **19** seemed to be a little bigger. After all, the overall performance of the model results in a satisfactory prediction for the activity tendency of the tested compounds.

Tab 3. Predictions of pIC_{50} values of test compounds compared to experimental data.

Test set	pIC_{50} (exptl)	pIC_{50} (pred)	Residual
17	1.74	1.60	0.14
18	1.45	1.67	-0.22
19	1.08	1.31	-0.23

DISCUSSION

3D-QSAR model was used to predict the antitumor effect of beta-carboline analogs, and the CoMFA analysis was used successful in this report. The CoMFA applied to the final alignment resulted in a q^2_{cv} of 0.656

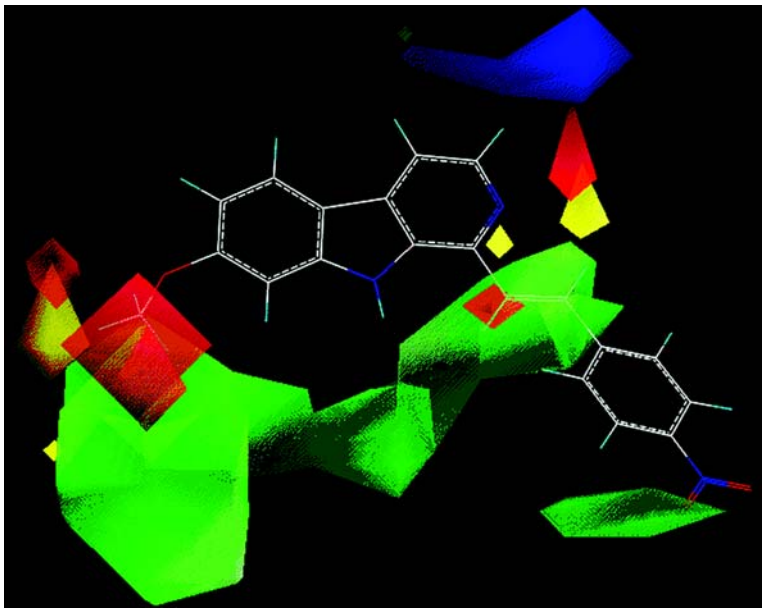

Fig 2. Graphical representation of the final CoMFA field. The color coding of the areas is as follows: red areas are the regions where negative potential is favorable for the pIC_{50} while blue ones are the regions where negative potential is unfavorable; green area mean steric favored and yellow area mean steric unfavored.

and it showed that the steric fields contributed 43.3 % of the model information while the electrostatic fields represented the other 56.7 %. It means that the model is reliable and the electrostatic fields affect the cytotoxities more to the model than the steric fields do. Also the model shows some principles about the 3D-QSAR of beta-carboline. In R_3 area, the model favors sterically demanding groups. In R_5 and R_2 areas, steric contributions are unfavored. In R_2 area of the molecules, three red regions dominate the electrostatic field, representing that negative potential in the region is favorable for pIC_{50} values. But it can not come to a conclusion absolutely because the correlation of cytotoxities and structural parameters is such a progress that various factors was involved in, including electrostatic field, steric field, hydrophobe force field and so on.

The key to the goal of this study was the design of new compounds and, as a result, the design of the best CoMFA model in terms of prediction. The experimentally obtained beta-carbolines correlate well with the results of our theoretical CoMFA model, with residuals near zero. Compound **17**, **18**, and **19** are designed and synthesized based on the model. The modification is to join a sterically demanding group in R_3 area, or join a negative potential group in R_2 area and so on. They all fit the CoMFA model well. Still the model can be further refined by introducing more force fields into the analysis, such as hydrophobe force field.

ACKNOWLEDGMENT We are grateful to Dr Hualiang JIANG of Shanghai Institute of Metaria Medica of Chinese Academy of Sciences for his precious advices and supports on the CoMFA analysis, to Dr Gang CHEN and Dr Xiao-ming LUO and all the other colleagues of DDDC group in Shanghai Institute of Metaria Medica of Chinese Academy of Sciences for their valuable and warm help in our study.

REFERENCES

1 Xie Y, Luo TX. Study of tah-induced apoptosis in Hela cell. Tumor 1998; 18: 131-3.
2 Duan JN, Zhou RH, Zhao SX. Studies on the chemical constituents of peganum multisectum maxim I. The alkaloids from seeds and antitumour activity. J China Pharm Univ 1998; 29: 21-3.
3 Pan QC, Yang XP, Li CJ. Studies on the pharmacological action of the total alkaloid of peganum harmala. Acad J Sums 1997; 18: 165-7.
4 Wang XH, Wang H, He AG. Study on the antitumor effect of total harmala. J China Med Univ 1996; 25: 240-2.
5 Li GW, Liang PG, Pan GY. Radioprotective effect of γ-carboline and its carboline analogues. Acta Pharm Sin 1995; 30: 715-7.
6 Holmstedt B. Betacarbolines and tetrahydroisoquinolines: historical and ethnopharmacological background. Prog Clin Biol Res 1982; 90: 3-13.
7 Johnson FB. Chemical interactions with herpes simplex type 2 virus: enhancement of transformation by norharman. Carcinogenesis 1982; 3: 457-9.
8 Mita S, Kamataki T, Kat R. Effect of norharman on DNA strand breaks and mutation of Chinese hamster V79 cells by chemical carcinogens. Carcinogenesis 1984; 5: 715-8.
9 Sasak YF, Yamada H, Shimoi K, Kinae N, Tomita I, Matsumura H, *et al*. Enhancing effects of heterocyclic amines and beta-carbolines on the induction of chromosome aberrations in cultured mammalian cells. Mutat Res 1992; 269: 79-95.
10 Mactutus CF, Tilson HA. Evaluation of long-term consequences in behavioral and/or neural function following neonatal chlordecone exposure. Teratology 1985; 31: 177-86.
11 Zajdela F, Perin-Roussel O, Saguem S. Marked differences between mutagenicity in Salmonella and tumour-initiating activities of dibenzo [a,e]fluoranthene proximate metabolites; initiation inhibiting activity of norharman. Carcinogenesis 1987; 8: 461-4.
12 Wakabayashi K, Nagao M, Kawachi T, Sugimura T. Mechanism of appearance of mutagenicity of *N*-nitrosodiphenylamine with norharman. IARC Sci Publ 1982; 41: 695-707.
13 Ashby J, Elliott BM, Styles JA. Norharman and ellipticine: a comparison of their albilities to interact with DNA *in vitro*. Cancer Lett 1980; 9: 21-33.
14 Ohnishi S, Murata M, Oikawa S, Totsuka Y, Takamura T, Wakabayashi K, *et al*. Oxidative DNA damage by an *N*-hydroxy metabolite of the mutagenic compound formed from norharman and aniline. Mutat Res 2001; 25: 63-72.
15 Lee CS, Han ES, Jang YY, Han JH, Ha HW, Kim DE. Protective effect of harmalol and harmaline on MPTP neurotoxicity in the mouse and dopamine-induced damage of brain mitochondria and PC12 cells. J Neurochem 2000; 75: 521-31.
16 Hada N, Totsuka Y, Enya T, Tsurumaki K, Nakazawa M, Kawahara N, *et al*. Structures of mutagens produced by the co-mutagen norharman with o- and m-toluidine isomers. Mutat Res 2001; 27: 115-26.
17 Sasaki YF, Shirasu Y. Suppressing effects of S phase post-treatment with carbolines on sister-chromatid exchanges induced by mitomycin C in Chinese hamster cells. Mutat Res 1993; 302: 165-71.
18 Cramer RD III, Patterson DE, Bunce JD. Comparative molecular field analysis (CoMFA). 1. Effect of shape on binding of steroids to carrier proteins. J Am Chem Soc 1988; 110: 5959-67.
19 Ishidda J, Wang HK, Bastow KF, Hu CQ, Lee KH. Antitumor agents 201. Cytotoxicity of harmine and beta-carboline analogs. Bioorg Med Chem Lett 1999; 9: 3319-24.
20 Klebe G, Abraham U, Mietzner T. Molecular similarity indices in a comparative analysis (CoMSIA) of drug molecules to correlate and predict their biological activity. J Med Chem 1994; 37: 4130-46.

21 Clark M, Cramer RD III, van Opdenbosch N. Validation of the general purpose Tripos 5.2 force field. J Comput Chem 1989; 10: 982-1012.
22 Wang R, Gao Y, Lai L. All-orientation search and all-placement search in comparative molecular field analysis. J Mol Model 1998; 4: 276-83.
23 Dunn WJ, Wold S, Edlund V, Helberg S. Multivariate structure-activity relationships between data from a battery of PLS method. Quantum Struct-Act Relat 1984; 3: 131-7.
24 Lanig H, Utz W, Gmeiner P. Comparative molecular field analysis of dopamine D4 receptor antagonists including 3-[4-(4-Chlorophenyl)piperazin-1-ylmethyl] pyrazolo [1,5-α] pyridine (FAUC113),3-[4-(4-Chlorophenyl)piperazin-1-ylmethyl]-1H-pyrrolo-[2,3-β]pyridine(*L*-745,870), and clozapine. J Med Chem 2001; 44: 1151-7.
25 Newman AH, Izemwasser S, Robage MJ, Kline RH. CoMFA study of novel phenyl ring-substituted 3α-(diphenylmethoxy) tropanes analogues at the dopamine transporter. J Med Chem 1999; 42: 3502-9.
26 Han R, editor. Research and development of anticancer drugs and experimental techniques. 1st ed. Peking: Peking Union Medical College Publishing Company; 1997. p 284-6.